amiodarone 100 mg dailyis started [9]. Conversely, amiodarone withdrawal can lead to under-anticoagulation, and therefore to an increased risk of thrombosis.

In conclusion, we describe the first case of genetic VKA resistance in a child who had the p.Asp36Tyr mutation combined with g.−1185G>A and g.−679A>G mutations in the 5′-flanking region. VKA resistance was partially masked initially by concomitant amiodarone therapy. Both warfarin–drug interactions and genetic variations should be considered in the management of VKA therapy. Physicians should be aware that potentially interfering drugs can increase or decrease the INR when they are introduced or withdrawn in patients on warfarin therapy. Close INR monitoring is advisable in such situations. Pharmacodynamic VKA resistance resulting from genetic factors may be masked by concomitant drugs.

Disclosure of Conflict of Interests

The authors state that they have no conflict of interest.

References

1 Monagle P, Chan AK, Goldenberg NA, Ichord RN, Journeycake JM, Nowak-Gottl U, Vesely SK. Antithrombotic Therapy in Neonates and Children: Antithrombotic Therapy and Prevention of Thrombosis, 9th ed: American College of Chest Physicians Evidence-Based Clinical Practice Guidelines. *Chest* 2012; **141**: e737S–801S.

2 Moreau C, Bajolle F, Siguret V, Lasne D, Golmard JL, Elie C, Beaune P, Cheurfi R, Bonnet D, Loriot MA. Vitamin K antagonists in children with heart disease: height and VKORC1 genotype are the main determinants of the warfarin dose requirement. *Blood* 2012; **119**: 861–7.

3 Watzka M, Geisen C, Bevans CG, Sittinger K, Spohn G, Rost S, Seifried E, Muller CR, Oldenburg J. Thirteen novel VKORC1 mutations associated with oral anticoagulant resistance: insights into improved patient diagnosis and treatment. *J Thromb Haemost* 2010; **9**: 109–18.

4 Bodin L, Perdu J, Diry M, Horellou MH, Loriot MA. Multiple genetic alterations in vitamin K epoxide reductase complex subunit 1 gene (VKORC1) can explain the high dose requirement during oral anticoagulation in humans. *J Thromb Haemost* 2008; **6**: 1436–9.

5 Pautas E, Moreau C, Gouin-Thibault I, Golmard JL, Mahe I, Legendre C, Taillandier-Heriche E, Durand-Gasselin B, Houllier AM, Verrier P, Beaune P, Loriot MA, Siguret V. Genetic factors (VKORC1, CYP2C9, EPHX1, and CYP4F2) are predictor variables for warfarin response in very elderly, frail inpatients. *Clin Pharmacol Ther* 2010; **87**: 57–64.

6 Klein TE, Altman RB, Eriksson N, Gage BF, Kimmel SE, Lee MT, Limdi NA, Page D, Roden DM, Wagner MJ, Caldwell MD, Johnson JA. Estimation of the warfarin dose with clinical and pharmacogenetic data. *N Engl J Med* 2009; **360**: 753–64.

7 Rost S, Fregin A, Ivaskevicius V, Conzelmann E, Hortnagel K, Pelz HJ, Lappegard K, Seifried E, Scharrer I, Tuddenham EG, Muller CR, Strom TM, Oldenburg J. Mutations in VKORC1 cause warfarin resistance and multiple coagulation factor deficiency type 2. *Nature* 2004; **427**: 537–41.

8 Kurnik D, Qasim H, Sominsky S, Markovits N, Li C, Stein CM, Halkin H, Gak E, Loebstein R. Effect of VKORC1D36Y variant on warfarin dose requirement and pharmacogenetic dose prediction. *Thromb Haemost* 2012; **108**: 781–8.

9 Sanoski CA, Bauman JL. Clinical observations with the amiodarone/warfarin interaction: dosing relationships with long-term therapy. *Chest* 2002; **121**: 19–23.

10 Holbrook AM, Pereira JA, Labiris R, McDonald H, Douketis JD, Crowther M, Wells PS. Systematic overview of warfarin and its drug and food interactions. *Arch Intern Med* 2005; **165**: 1095–106.

11 Lu Y, Won KA, Nelson BJ, Qi D, Rausch DJ, Asinger RW. Characteristics of the amiodarone–warfarin interaction during long-term follow-up. *Am J Health Syst Pharm* 2008; **65**: 947–52.

Structure and mechanics of fibrin clots formed under mechanical perturbation

S. MÜNSTER,*‡§ L. M. JAWERTH,† B. FABRY‡§ and D. A. WEITZ*†

**School of Engineering and Applied Sciences, Harvard University; †Department of Physics Harvard University, Cambridge, MA, USA; ‡Department of Physics, University Erlangen-Nuremberg; and §Max-Planck-Institute for the Science of Light Erlangen, Germany*

To cite this article: Münster S, Jawerth LM, Fabry B, Weitz DA. Structure and mechanics of fibrin clots formed under mechanical perturbation. *J Thromb Haemost* 2013; **11**: 557–60.

Correspondence: Stefan Münster, Department of Physics, Center for Medical Physics and Technology, University of Erlangen-Nuremberg, Henkestr. 91, 91052 Erlangen, Germany.
Tel.: +49(9131)8525602; fax: +49(9131)8525601.
E-mail: stefan@stefanmuenster.de

DOI: 10.1111/jth.12123

Received 24 October 2012, accepted 23 December 2012

The mechanical properties of a blood clot are of crucial importance for its ability to stem the flow of blood at a site of vascular injury [1]. These properties are largely determined by the mechanics of the underlying structural scaffold, a branched network of the biopolymer fibrin [1]. This network forms during coagulation, when monomeric fibrin assembles into protofibrils that laterally aggregate

into thicker fibers and occasionally branch to form a percolated, three-dimensional structure [2]. Alterations in network structure, such as changes in fiber density, fiber thickness or branching probability, strongly affect the mechanics of the network [3–6].

Investigations of the relationship of the network architecture to bulk-level mechanics are commonly performed on *in vitro* fibrin networks polymerized under static conditions [3,7,8]. However, in the body, blood clots form in a mechanically dynamic environment: intravascular clots form in the presence of flowing blood, whereas clots forming in the extravascular tissue might also be exposed to mechanical perturbations other than flow, for instance due to the action of breathing and body movements, or the pulsatile dilation of the vessel wall. Indeed, the structure of fibrin clots polymerized under fluid flow is profoundly changed [9,10]. However, the effects of mechanical perturbations during clot polymerization on clot structure and its resultant mechanical properties remain unknown.

Here, we report the effect of mechanical perturbation during polymerization on the structure and mechanics of fibrin clots. We polymerized fibrin clots (0.8 mg/mL human fibrinogen (Enzyme Research Labs, South Bend, IN, USA), 0.05 NIH units/mL human α-thrombin (Enzyme Research Labs), in a buffer containing 0.15 M NaCl, 20 mM Ca, 25 mM HEPES at pH 7.4) for at least 1 hour at 25 °C *in situ* in a strain-controlled rheometer (ARES-G2, TA Instruments, New Castle, DE, USA) fitted with a cone-plate geometry (Fig. 1A). During polymerization, we continuously applied sinusoidal shear perturbations with a frequency of 0.1 Hz at six different strain amplitudes (0%, 10%, 30%, 45%, 60% and 90%) (Fig. 1B). Subsequently, we measured the stress-strain response of the clots by applying a strain ramp at 1%/s (Fig. 1B). The local slope of the stress-strain curve characterizes the differential stiffness, K', of the material as a function of strain. All data are averages of two to four independent experiments per condition. We confirmed by denaturing gel electrophoresis that our fibrinogen stock had sufficient trace amounts of factor XIII for complete γ-γ cross-linking within 10 min, and that monomeric α-chains were nearly completely depleted after 1 hour of polymerization (data not shown).

Fibrin clots polymerized in the absence of mechanical perturbation exhibited a highly non-linear mechanical response with several characteristic regimes [8]. At low strain, the differential stiffness was constant, corresponding to a linear elastic modulus. Beyond a characteristic strain, the differential stiffness steeply increased and the mechanics became highly non-linear. Eventually, the differential stiffness reached a plateau and the mechanics became approximately linear. Ultimately, the differential stiffness again increased, with the mechanics again becoming non-linear until the clot broke (Fig. 1C).

Fibrin clots polymerized under oscillatory perturbations also exhibited these regimes. However, the characteristic strain for the onset of non-linearity increased with increasing perturbation amplitude (Fig. 1C, horizontal arrow). Interestingly, the transition into the plateau regime occurred at the strain value corresponding to the perturbation amplitude (Fig. 1C, vertical bars). Consequently, all further transitions were shifted to larger strains, and the clots ruptured successively later (Fig. 1D, blue). Moreover, the differential stiffnesses and the rupture stresses were of comparable magnitude for clots polymerized at perturbation amplitudes up to 60% (Fig. 1D, red). However, the initial stiffnesses in the linear regime decreased dramatically for perturbation amplitudes larger than 10% (Fig. 1D, green). These results suggest that the linear modulus, commonly reported as the only measure of clot mechanics, is a poor indicator of the high-strain mechanics and rupture stress.

To determine the origin of these perturbation-induced mechanical alterations, we polymerized fluorescently labeled fibrin clots (0.8 mg/mL of a 1:6 mixture of fibrinogen labeled with TAMRA-SE (Sigma, St Louis, MO, USA) with unlabeled fibrinogen) in a home-built parallel-plate shear cell mounted on a confocal microscope (Leica SP5, equipped with a 63 ×/1.2NA water immersion lens; Wetzlar, Germany) (Fig. 1E). To replicate the perturbing oscillations of the rheometer, we continuously moved the upper plate back and forth at different amplitudes for at least 1 hour while the clots were forming. Subsequently, we imaged the full three-dimensional structure of each clot by acquiring a stack of evenly spaced optical sections. Projections of x–z slices along the *y*-axis show that fibrin clots formed without perturbations had a largely homogeneous distribution of isotropically orientated fibers (Fig. 1F). In contrast, the structure of clots polymerized under perturbation showed two distinct layers: a layer of homogeneous clot structure with a density comparable to that of the unperturbed sample, and a second layer with a highly inhomogeneous structure of bundled fibers and large pores (Fig. 1H–J). The thickness of the bundled layer increased with increasing perturbation amplitude, and the pore size was comparable to the layer thickness. Similar fiber bundling has also been reported for networks polymerized under steady fluid flow [10]. Layer formation and bundling occurred only when the perturbations were applied during polymerization; to confirm this, we applied an oscillatory strain of 60% for 1 hour to a clot polymerized under static conditions. We found that the fiber density and degree of homogeneity of the clot remained unchanged (Fig. 1G). Moreover, the non-linear mechanics of fully polymerized and cross-linked clots did not change even under repeated large shear oscillations (data not shown) [11].

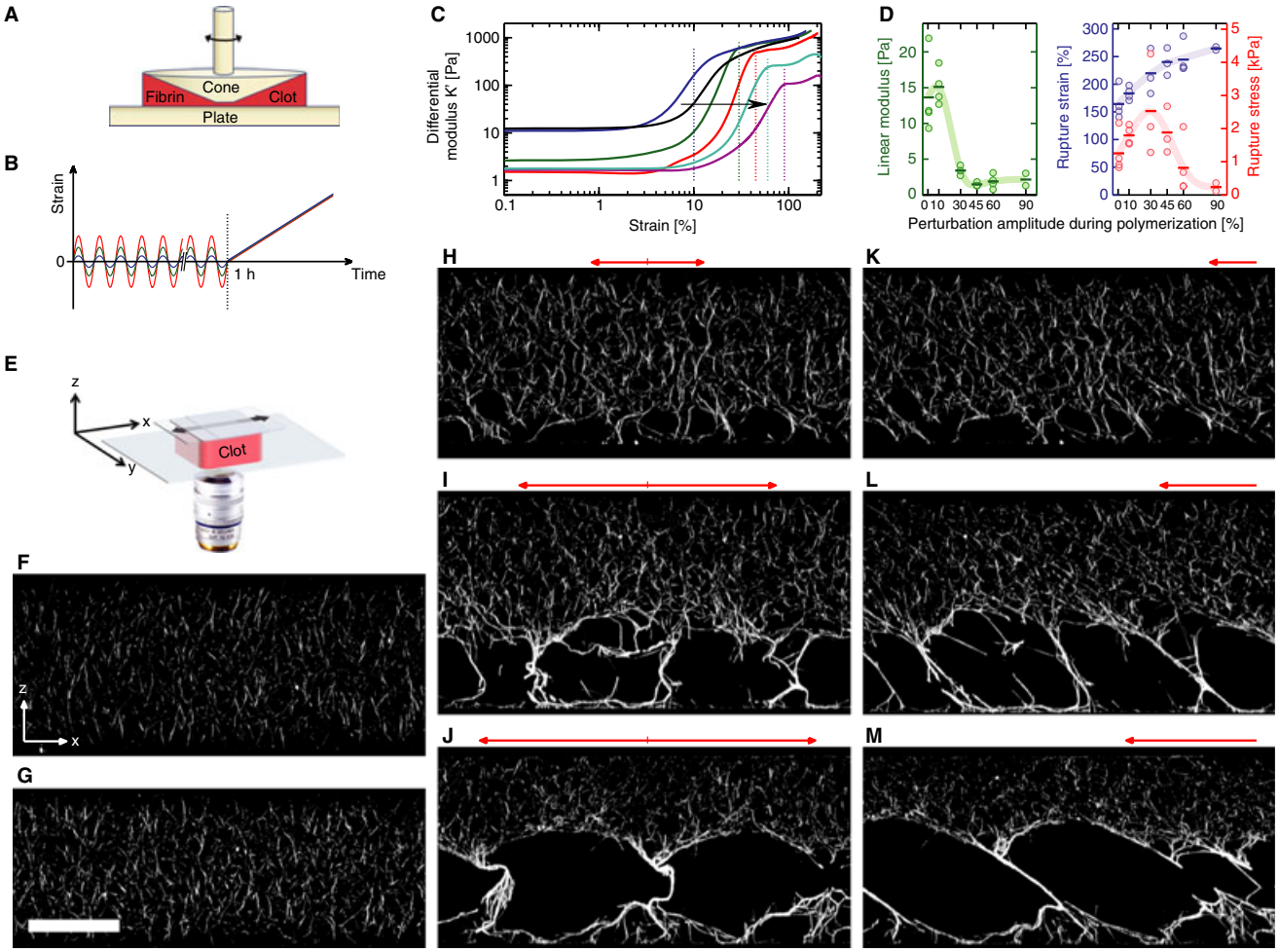

Fig. 1. Mechanical properties and three-dimensional structure of fibrin clots polymerized under oscillatory shear deformations of different amplitudes. (A) Bulk rheological measurements were performed in a strain-controlled rheometer fitted with a cone-plate geometry. (B) Test protocol: continuous shear oscillations of 0.1 Hz at various amplitudes (blue, green and red) were applied for one hour; subsequently, strain ramps at 1%/s were applied to measure the stress-strain relationship. (C) Log-log plot of the differential modulus K' vs. strain of clots formed without perturbation (black) and with perturbations of 10% (blue), 30% (green), 45% (red), 60% (turquoise) and 90% (purple) strain amplitude. Colored vertical bars mark the strain amplitude of the perturbation at which the samples were polymerized. Clots polymerized under larger perturbation amplitudes exhibited a consistently later onset of strain-stiffening (horizontal arrow). (D) Linear modulus (green), rupture strain (blue) and rupture stress (red) for all samples. Circles depict the values of each individual measurement, and horizontal bars represent averages per condition. Light colored lines are added to guide the eye. (E) Fluorescently labeled fibrin networks were polymerized in a shear cell consisting of two parallel glass plates on a confocal microscope while the upper plate oscillated at different amplitudes horizontally with a period of 10 s. Similarly, in panels F–M, the bottom plate was the stationary glass plate of the shear cell, whereas the top plate was moved by the actuator (as shown by the coordinate systems in panel F, which corresponds to panel E and applies to panels G–M alike). (F–J) Maximum projections along the *y*-axis spanning 33 μm in depth depict the resulting structure of the fibrin networks in their 0% strain position. (F) Structure of a clot formed without perturbations. (G) Structure of a clot polymerized without perturbations after oscillatory shear deformations of 60% strain amplitude have been imposed for 1 hour. The scale bar of 100 μm applies equally to panels F–M. (H–J) Structure of clots polymerized under perturbations. Red arrows indicate the amplitude of the motion of the top plate during polymerization (same scale as scale bar in G; corresponding to 30%, 60% and 90% strain amplitude). (K–M) Maximum projections (taken from movie S1 in the Supporting Material) of the networks from H–J under shear; the strain values shown depict the points at which the bundled regions became straight and the upper dense regions just began to deform. Red arrows indicate the displacement of the top plate at these strain values (corresponding to strains of 25%, 45% and 75%).

To explore how the change in clot structure led to changes in the mechanical response, we translated the top plate by 5% strain increments and acquired full three-dimensional images after each shear step. The sequence of x–z projections reveals the dynamic behavior of the clots as they were sheared (movie S1 in Supporting Material). A clot polymerized under static conditions deformed evenly throughout its entire thickness, with many fibers aligning in the direction of strain; in the strain-stiffening regime, these fibers stretched homogeneously, suggesting that the mechanical properties are homogenous throughout the clot. In contrast, for the clots polymerized under oscillatory perturbation, the two structurally different layers exhibited different behaviors when the clots were

sheared (movie S1). Initially, at low strains, the fiber bundles accommodated the full applied deformation by tilting and straightening, whereas the fibers in the dense region remained virtually undeformed and only translated horizontally with the moving plate. However, once the fiber bundles became straight, the dense region of the clot also began to deform.

Clots polymerized under larger perturbation amplitudes had larger regions of thicker yet more undulated bundles, which could accommodate a proportionally larger deformation until they were straightened; hence, the strain where the denser region began to stretch was greater (Fig. 1K–M). Furthermore, the lowered linear modulus of these clots indicates that the initial straightening of the bundles required less force than the deformation of unperturbed clots. However, once the fiber bundles were straightened and the clots exhibited strain-stiffening, the typical stiffness range was comparable to that of unperturbed clots. Hence, the mechanics of the dense region of perturbed clots must be similar to those of unperturbed clots. Therefore, the occurrence of the structural heterogeneity explains the delayed onset of the non-linear stiffening of clots formed under perturbation, whereas the abundance of a dense clot layer explains the mechanical similarity to unperturbed clots when strained to large deformations.

In contrast to undulated bundles formed upon application of oscillatory perturbations during polymerization, application of a constant flow during polymerization of fibrin clots results in straight fibers aligned in the direction of flow [9,10]. Undulated bundles led to a lower linear modulus and a delay in the non-linear response; in contrast, straight fibers should cause an immediate onset of the non-linear response, which would increase the apparent linear modulus of clots formed under flow [10].

In conclusion, we have shown that fibrin polymerized under continuous oscillatory shear perturbations forms rigid clots that exhibit a significantly later onset of strain-stiffening, a postponed rupture strain, and a lower linear modulus. Up to perturbation amplitudes of 45% strain, the typical non-linear stiffnesses of these clots, as well as their rupture stresses, are of similar magnitude to those formed without perturbation. These changes in the mechanical properties result from changes in clot architecture: one part of the clot shows a highly bundled structure, while the remaining part is virtually unaltered. This architectural adjustment to the specific loading conditions of the environment may enable blood clots to maintain their non-linear properties and prevent early rupture, hence, allowing them to serve their function over a wide range of mechanical challenges.

Acknowledgements

This work was supported by the 'Emerging Fields Initiative' of the University of Erlangen-Nuremberg (Project: TOPbiomat) (SM and BF) and by the National Science Foundation through the Harvard Materials Research Science and Engineering Center (DMR-0820484) (DAW).

Disclosure of Conflict of Interests

The authors state that they have no conflict of interest.

Supporting Information

Additional Supporting Information may be found in the online version of this article:

Movie S1. Dynamic behavior of fibrin clots polymerized under perturbation during shear up to 250% strain in 5% increments.

References

1 Weisel JW. The mechanical properties of fibrin for basic scientists and clinicians. *Biophys Chem* 2004; **112**: 267–76. 10.1016/j.bpc.2004.07.029.
2 Chernysh IN, Nagaswami C, Weisel JW. Visualization and identification of the structures formed during early stages of fibrin polymerization. *Blood* 2011; **117**: 4609–14. 10.1182/blood-2010-07-297671.
3 Ryan EA, Mockros LF, Weisel JW, Lorand L. Structural origins of fibrin clot rheology. *Biophys J* 1999; **77**: 2813–24. 10.1016/s0006-3495(99)77113-4.
4 Fatah K, Silveira A, Tornvall P, Karpe F, Blomback M, Hamsten A. Proneness to formation of tight and rigid fibrin gel structures in men with myocardial infarction at a young age. *Thromb Haemost* 1996; **76**: 535–40.
5 Collet JP, Woodhead JL, Soria J, Soria C, Mirshahi M, Caen JP, Weisel JW. Fibrinogen dusart: electron microscopy of molecules, fibers and clots, and viscoelastic properties of clots. *Biophys J* 1996; **70**: 500–10.
6 Wolberg AS, Aleman MM. Influence of cellular and plasma procoagulant activity on the fibrin network. *Thromb Res* 2010; **125**: S35–7. 10.1016/j.thromres.2010.01.033.
7 Chernysh IN, Weisel JW. Dynamic imaging of fibrin network formation correlated with other measures of polymerization. *Blood* 2008; **111**: 4854–61. 10.1182/blood-2007-08-105247.
8 Piechocka IK, Bacabac RG, Potters M, MacKintosh FC, Koenderink GH. Structural hierarchy governs fibrin gel mechanics. *Biophys J* 2010; **98**: 2281–9. 10.1016/j.bpj.2010.01.040.
9 Gersh KC, Edmondson KE, Weisel JW. Flow rate and fibrin fiber alignment. *J Thromb Haemost* 2010; **8**: 2826–8. 10.1111/j.1538-7836.2010.04118.x.
10 Campbell RA, Aleman MM, Gray LD, Falvo MR, Wolberg AS. Flow profoundly influences fibrin network structure: implications for fibrin formation and clot stability in haemostasis. *Thromb Haemost* 2010; **104**: 1281–4. 10.1160/th10-07-0442.
11 Kang H, Wen Q, Janmey PA, Tang JX, Conti E, MacKintosh FC. Nonlinear elasticity of stiff filament networks: strain stiffening, negative normal stress, and filament alignment in fibrin gels. *J Phys Chem B* 2009; **113**: 3799–805. 10.1021/jp807749f.